THE EFFECT OF THE 1991–1993 ENSO ON THE CALIFORNIA CURRENT SYSTEM

RONALD J. LYNN
Southwest Fisheries Science Center
National Marine Fisheries Service
P.O. Box 271
La Jolla, California 92038

FRANKLIN B. SCHWING
Pacific Fisheries Environmental Group
Southwest Fisheries Science Center
National Marine Fisheries Service
1352 Lighthouse Avenue
Pacific Grove, California 93950

THOMAS L. HAYWARD
Marine Life Research Group
Scripps Institution of Oceanography
University of California, San Diego
La Jolla, California 92093-0227

ABSTRACT

During 1992 and 1993 the coastal zone of the eastern North Pacific Ocean experienced widespread sea-surface warming (1°–2°C) and, for extended periods, higher-than-normal sea level (5–14 cm) and unseasonably strong poleward coastal currents. These are manifestations of an El Niño event as it affects the California Current system (CCS). The warm phase of the tropical El Niño–Southern Oscillation (ENSO) started in the fall of 1991 and, after the expected lag of several months, was evidenced in the CCS. Hayward (1993) and Hayward et al. (1994) give a preliminary look at the oceanographic effects of the 1991–92 event off California. We update these reports and present additional results from hydrographic surveys and coastal time series data. Comparisons are made with prevailing large-scale meteorological conditions. There is evidence that these El Niño conditions resulted from a combination of remote and local atmospheric forcing. Midyear reversals in anomalous coastal poleward currents and in corresponding high sea levels toward more typical conditions (equatorward flow, near zero sea-level anomalies) were followed by the renewal of positive anomalous sea level. The intra-annual pulsing of the current field and sea level observed during 1992 characterized the 1957–58 El Niño as well. This pattern also bears a strong resemblance to numerical model results, thus giving evidence for the development of a poleward-propagating coastal Kelvin wave and offshore-directed Rossby waves generated by El Niño.

INTRODUCTION

Like previous moderate-to-strong ENSO events, the 1991–93 ENSO had a substantial effect far beyond the equatorial zone. The physical impact of ENSO events upon the California Current system (CCS) and the Pacific Northwest have been described by many authors (e.g., Emery and Hamilton 1985; Mysak 1986; Simpson 1984, 1992; see also Wooster and Fluharty 1985). Typically, the oceanic effects in the CCS include widespread and intensive warming of the upper mixed layer, a depressed thermocline and nutricline, anomalously high sea level, an enhanced poleward countercurrent along the continental margin, and significant but varied effects on the marine biota. These effects were found along much of the west coast of North America during 1992 and 1993, and selected evidence is presented herein. The extensive and persistent nature of the sea-surface warming is illustrated in the *Climate Diagnostics Bulletin* series 1992 through June 1994. Hayward (1993) and Hayward et al. (1994) give a preliminary look at the oceanographic effects of the 1991–92 episode, including the sea-level anomalies. The purpose of this report is to describe the anomalous physical changes in the CCS during the 1991–93 ENSO event as indicated in hydrographic surveys and coastal time series data. We focus on the region's circulation, which is implied by dynamic height anomalies.

BACKGROUND

Enfield and Allen (1980) and Chelton and Davis (1982) show that sea-level fluctuations at ENSO frequencies propagate poleward along the west coast of the American continents. These observations have been used to support the concept that El Niño conditions off the U. S./Canadian west coast are linked to equatorial ENSO events by coastally trapped waves emanating from the eastern Pacific equatorial zone along the continental margin. But not all equatorial ENSO events have counterparts in the eastern subtropical Pacific, and vice versa. Simpson (1983) and Mysak (1986) provide strong arguments that large-scale anomalies in the winter barometric pressure field over the North Pacific and the resulting atmospheric circulation can better account for the occurrence of El Niño conditions off North America. Such anomalous atmospheric patterns have teleconnections to the Southern Oscillation (Horel and Wallace 1981) and match the spatial scale of SST anomalies. Theoreticians, however, continue to develop increasingly sophisticated wind-driven models that suggest the remote generation of energy and its propagation poleward along eastern ocean boundaries (e.g., Clarke and Van Gorder 1994; Jacobs et al. 1994).

Using a 34-year record of monthly mean temperature in the upper 300 meters of the eastern North Pacific (within 300 km of the coast), Norton and McLain (1994) proposed a method to distinguish between the dominance of local and remote forcing for El Niño events. Large, positive thermal anomalies that extend to 300 m correlate best to remote forcing (Southern Oscillation/coastally trapped wave propagation), whereas large anom-

alies limited to shallow depths correlate to local forcing (enhanced Aleutian low). The deeper-level warming along the coast is partially attributable to geostrophic adjustment to the increase in poleward flow, which is caused by the coastally trapped baroclinic Kelvin wave. Increased advection from the south may further contribute to the positive temperature anomaly of the water column. On the other hand, anomalous atmospheric forcing over the eastern North Pacific may significantly decrease upwelling-favorable wind stress (or increase downwelling-favorable wind stress) in the coastal regions. This condition causes unseasonably high surface-layer temperatures, but its effects below 100 m may be weaker than those caused by the remote forcing. Anomalies in the CCS are largest in those events in which both remote and local forcing are strong (e.g., 1940–41 and 1982–83).

Other large-scale processes may complicate the El Niño model. Latif and Barnett (1994) describe a cycle of large-scale sea-surface temperature (SST) patterns involving unstable air-sea interactions between the subtropical gyre circulation in the North Pacific and the Aleutian low-pressure system. In their model the SST in a large region of the central and western North Pacific (including the Kuroshio Extension) oscillates irregularly between positive and negative anomalies on a decadal time scale. The extensive warming of surface waters along the North American coast that occurs during strong El Niño events is part of this larger pattern that includes large-scale negative SST anomalies in the central North Pacific (Mysak 1986). In another study, Jacobs et al. (1994) used satellite altimeter observations to detect the northwestward progression over the last decade of a Rossby wave originally excited by the 1982–83 El Niño. Its impingement on the Kuroshio Extension during 1992–93 also has implications for the large-scale gyre circulation and the recent SST anomaly pattern. A simple model of the forcing of events in the eastern North Pacific may not be an appropriate approach.

Observations are inadequate for a clear understanding of the forcing of anomalous conditions along the North American coast. A modest number of hydrographic surveys conducted during 1992–93 describe conditions at various stages of development. The listing of cruises in table 1 was assembled from a general knowledge of ship activity and is not intended to be complete. Only a few of these surveys are treated in this report; however, the results are representative of seasonal patterns in the regional ENSO signal.

OBSERVATIONS

Characteristically, El Niño warming in the eastern North Pacific occurs in the fall–winter following the summer–fall development of ENSO changes in the tropics. Early suggestions of a developing ENSO were noted in the July and August 1991 issues of *Climate Diagnostics Bulletin*. Tropical ENSO conditions ensued across the equatorial Pacific in the subsequent months. Despite this, the coastal zone waters of the eastern North Pacific (Vancouver Island to southern Baja California) were cooler than seasonal norms from the spring of 1991 through the remainder of the year (*Oceanographic Monthly Summary* series). Large coastal regions had anomalies of $-1°$ to less than $-2°$C in June through September 1991. The magnitude of the cool anomalies diminished in late 1991. By February 1992, continued ocean warming produced significant widespread positive SST anomalies along the entire North American coastal zone, and offshore to distances greater than 1000 km.

TABLE 1
1992–93 Surveys (CTD/ADCP) off California

Dates	Vessel	Spatial extent	Reference
1/28–2/13/92	*Jordan*	CalCOFI pattern	SIO 1992b
2/7–2/17/92	*Pt. Sur*	37.2–38°N, to 123.5°W	Jessen et al. 1992
2/23–3/6/92	*Jordan*	36.8–38.3°N, to 126°W	Sakuma et al. 1994a
3/14–4/2/92	*Jordan*	37–38.8°N, to 128.5°W	Lynn et al. (data rep., in prep.)
4/13–4/30/92	*Jordan*	CalCOFI pattern	SIO 1992b
5/11–5/19/92	*Jordan*	36.5–38.3°N, to 124.8°W	Sakuma et al. 1994a
5/19–5/26/92	*Jordan*	36.5–38.3°N, to 124°W	Sakuma et al. 1994a
6/4–6/16/92	*Jordan*	36.5–38.3°N, to 126°W	Sakuma et al. 1994a
7/24–8/9/92	*Jordan*	CalCOFI pattern	SIO 1992a
9/28–10/14/92	*N Horizon*	CalCOFI pattern	SIO 1992a
1/12–1/27/93	*Jordan*	CalCOFI pattern	SIO 1993
3/2–3/13/93	*Jordan*	36.5–38.5°N, to 127°W	Sakuma et al. 1994b
3/30–4/15/93	*Jordan*	CalCOFI pattern	SIO 1993
5/13–5/20/93	*Jordan*	36.5–38.3°N, to 124°W	Sakuma et al. 1994b
5/21–5/28/93	*Jordan*	36.5–38.3°N, to 124°W	Sakuma et al. 1994b
6/3–6/10/93	*Jordan*	36.5–38.3°N, to 124°W	Sakuma et al. 1994b
6/5–7/13/93	*Wecoma*	36.2–39.5°N, to 128.5°W	Kosro et al. (data rep., in prep.)
7/8–7/12/93	*Jordan*	37.8–38.5°N, to 124.5°W	Lynn et al. (data rep., in prep.)
8/11–8/27/93	*N Horizon*	CalCOFI pattern	SIO 1994
8/14–9/21/93	*Wecoma*	37–39°N, to 128°W	Kosro et al. (data rep., in prep.)
10/8–10/26/93	*N Horizon*	CalCOFI pattern	SIO 1994

Central California Hydrographic Surveys, 1992

The CTD/Rosette survey from 14 March through 2 April 1992 by R/V *David Starr Jordan* (table 1) reached 500 km offshore and fell within the early period of coastal warming associated with this ENSO event. The dynamic height of the surface with respect to 500 dbar (figure 1a) reveals a region of poleward coastal countercurrent extending 200 km offshore. The deeper flow, as shown by the dynamic height at 250 m with respect to 500 dbar (figure 1b), shows the same broad poleward flow at half the surface velocity. Northward components of acoustic Doppler current profiler (ADCP) velocity exceeded 20 cm/s near 30 m depth and 10 cm/s at 200 m depth (P. M. Kosro, pers. comm.).

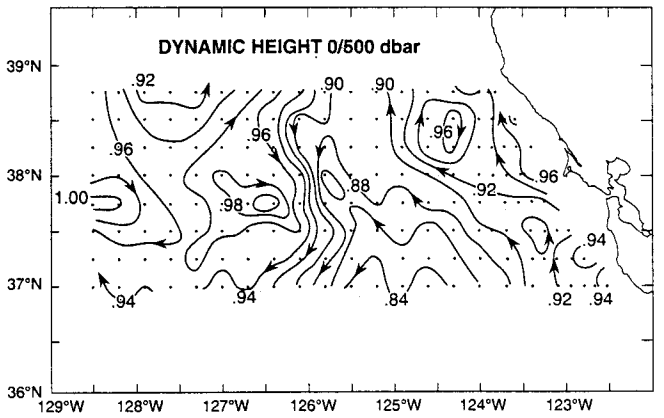

a

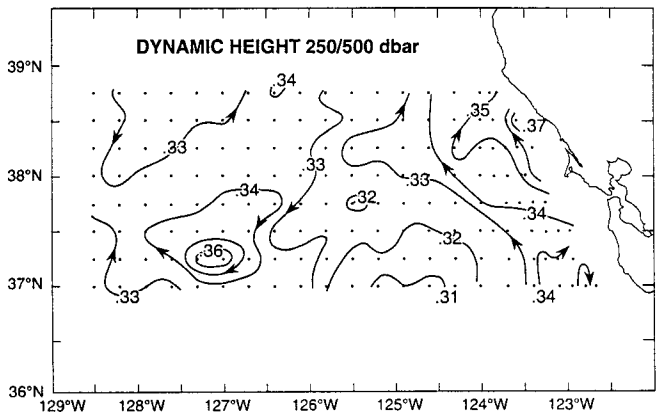

b

Figure 1. *a*, Dynamic height (dyn. m) of the surface with respect to 500 dbar for R/V *David Starr Jordan* survey, 14 March to 2 April 1992. Contour interval is .02 dyn. m. *Arrows* indicate direction of relative geostrophic flow. *b*, The same as *a*, except showing the 250 m level and with a contour interval of .01 dyn. m.

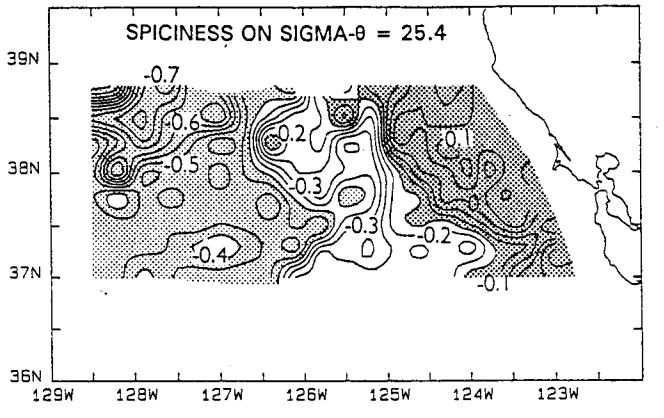

a

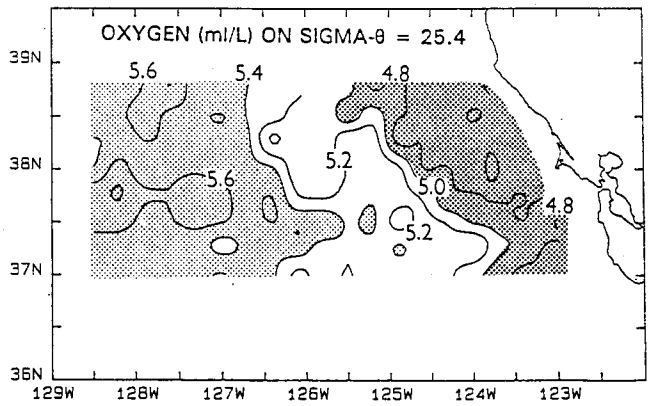

b

Figure 2. *a*, Spiciness on the surface where sigma-θ = 25.4 for survey shown in figure 1. Contour interval is 0.05. *b*, Same as *a*, except showing oxygen concentration (ml/l) and with a contour interval of 0.2.

Properties of the water mass have shown a high gradient in association with the jet of the California Current (Huyer et al. 1991; Strub et al. 1991). There is a high gradient in spiciness on the 25.4 sigma-θ surface in figure 2a that roughly aligns with the jet structure along the 126°W meridian (figure 1). Water to the west of the gradient has low spiciness (low temperature and low salinity) and is of northerly origin. A second gradient between 124° and 125°W (roughly parallel to the coastline) aligns with the outer portion of the strong poleward flow. Water shoreward of this gradient has the highest spiciness (highest temperature and highest salinity) on this density surface and is of southerly origin. A region of strong mixing is found between these two gradients. The distribution of oxygen concentration on this density surface shows a similar double gradient pattern (figure 2b), with lower oxygen concentrations associated with spicy, southern water (Lynn et al. 1982). Similar distribution patterns exist on other density surfaces; some have even stronger gradients (not shown). The vertical extent of this pattern is evidenced by the separation of envelopes about groupings of θ-S curves from stations in the coastal and offshore zones (figure 3). Except for the very-near-surface waters, these envelopes show little or no overlap for densities less than sigma-θ = 26.25 (nominally 370 m).

The survey described above was preceded by two surveys in the same region (table 1). In a survey aboard R/V *Pt. Sur* off the Gulf of the Farallones (7–17 February 1992) Ramp et al. (1992) found poleward near-surface ADCP velocities exceeding 40 cm/s. This contrasted with much weaker velocities and poleward flow limited to the slope (as opposed to the shelf) at the same location one year earlier. An ARGOS drifter drogued at 10 m and released in the gulf in February 1992 moved northward and onshore at speeds of 20–25 km/day (23–29 cm/sec) for about two weeks. In a more extensive survey (offshore to 126°W) conducted aboard the R/V *David Starr Jordan*, 24 February to 6 March, a flow pattern identical to the 14 March–2 April survey

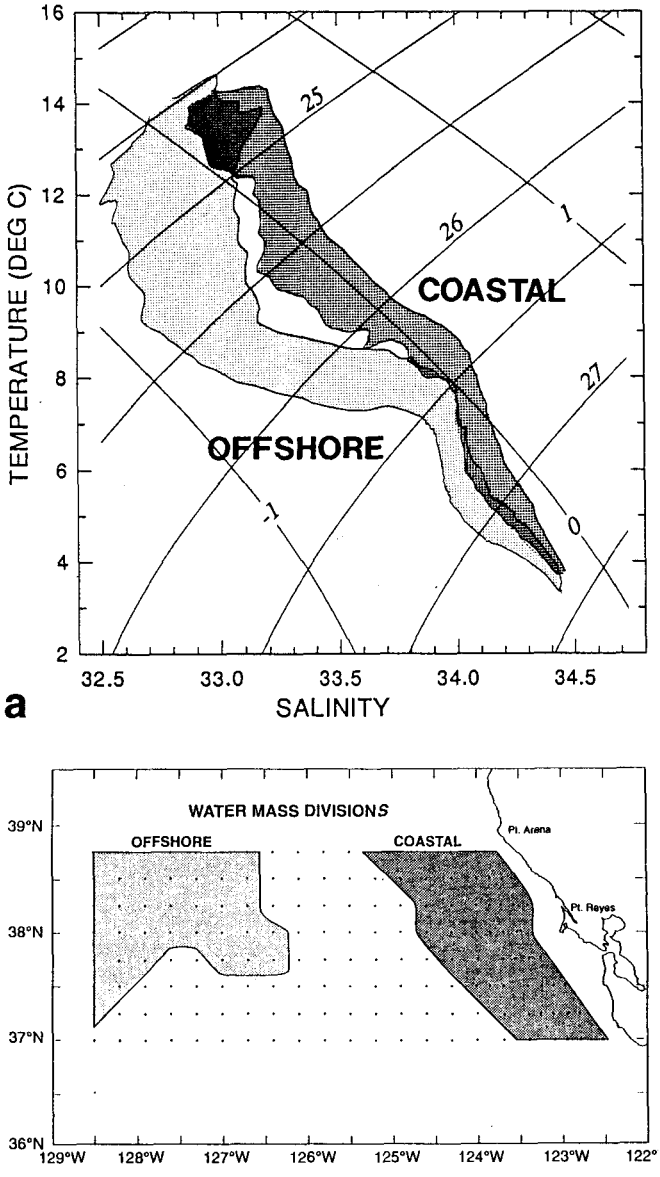

Figure 3. *a*, Envelopes about potential temperature-salinity (θ-S) curves (survey of figures 1 and 2) for coastal (*dark shading*) and offshore (*light shading*) waters. Curved lines slanting upward to the right are sigma-θ; lines slanting to the left are spiciness. *b*, Locations of coastal and offshore stations shown in *a*.

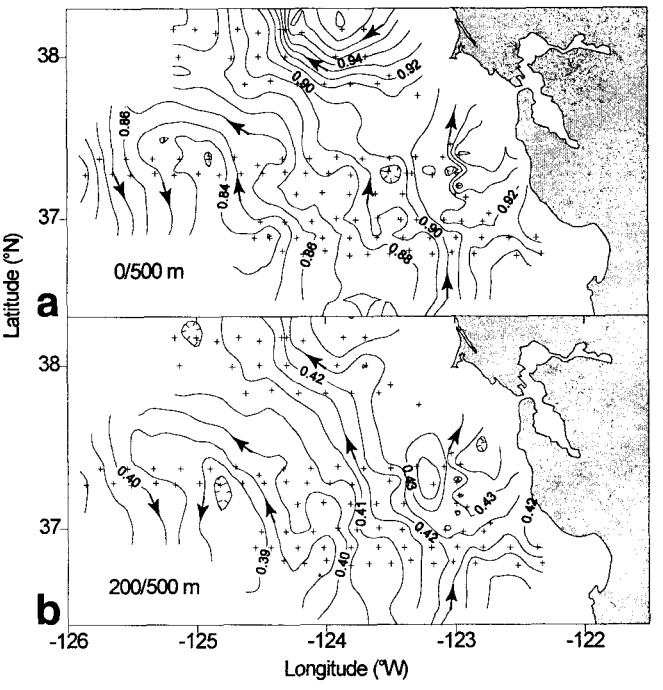

Figure 4. *a*, Dynamic height (dyn. m) of the surface with respect to 500 dbar for R/V *David Starr Jordan* survey, 23 February–March 6 1992. Contour interval is .01 dyn. m. *b*, Same as *a*, except showing the 200 m level and with a contour interval of 0.005 dyn. m.

(figure 1) was observed at the surface and at 200 m (figure 4); i. e., strong poleward flow along the coast and extending to 200 km offshore.

In the June 1992 R/V *David Starr Jordan* survey (table 1), portions of two CTD station lines taken in March (approximately 2.5 months earlier) were repeated, along with additional slope and shelf stations. No surface inshore countercurrent was found during the June period (figure 5a). The undercurrent at 500 m was confined to a narrow 50 km of the slope/shelf break (figure 5b). A comparison of water mass characteristics from late spring 1991 and 1992, represented by a station (37°N, 122.7°W) 37 km off Point Año Nuevo (figure 6), shows a warmer and less saline surface layer in 1992, and warmer and more saline waters on density surfaces in the pycnocline and deeper (to sigma-θ = 26.8; approximately 400 m). Although the May 1992 *Jordan* surveys did not cover as broad an offshore area (table 1), the circulation and water-mass distributions are very similar to those found in June.

Southern California (CalCOFI) Hydrographic Surveys, 1992

The dynamic heights of the surface with respect to 500 dbar for the February, April, July, and October 1992 CalCOFI surveys are given in figures 7–9; see also Hayward et al. (1994, 1995). The dynamic height for the 200 m level for February and April is also given in figures 7 and 8. The February 1992 pattern shows a strong and broad poleward countercurrent and undercurrent, which was highly anomalous when compared to Lynn and Simpson's (1987) long-term seasonal mean. By April 1992, surface currents were equatorward, in a pattern similar to the mean. The undercurrent at 200 m also disappeared by April and was replaced by a complex pattern of weak baroclinicity comparable to the mean. The July pattern of baroclinic flow was complicated by eddies, but did reveal a shoreward shift of a

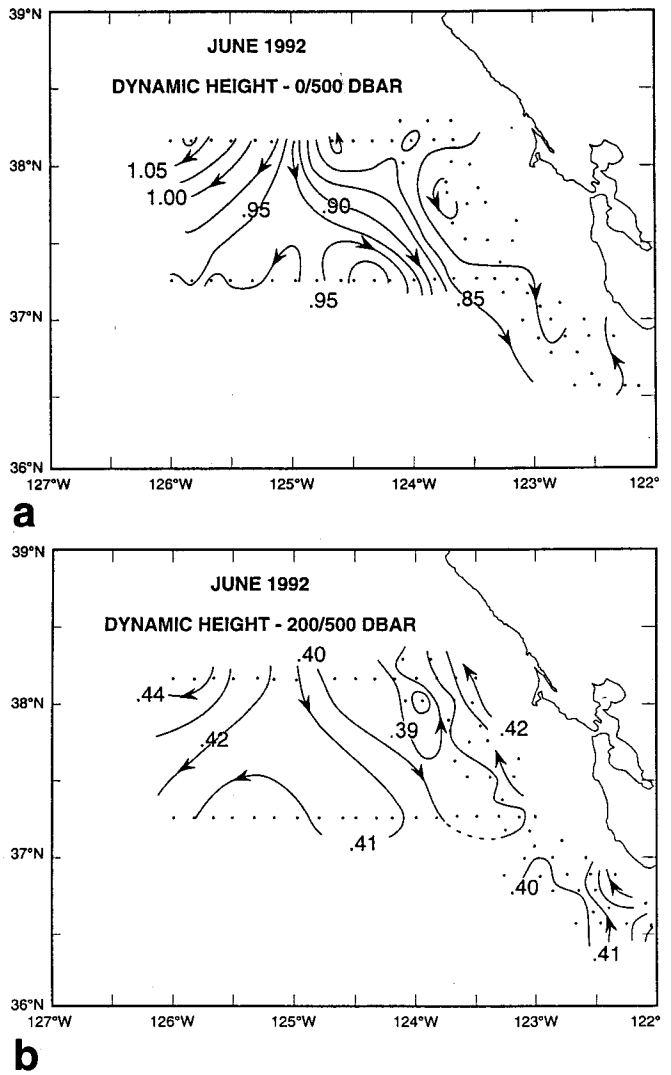

Figure 5. Dynamic height (dyn. m) of the surface with respect to 500 dbar for R/V *David Starr Jordan* survey of 4–10 June 1992. Contour interval is 0.025 dyn. m. *b*, Same as *a*, except showing the 200 m level and with a contour interval of 0.01 dyn. m.

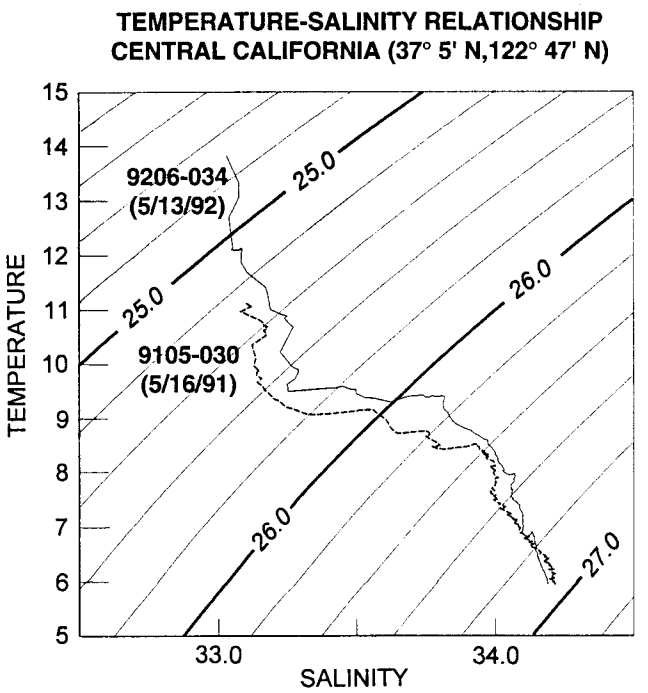

Figure 6. θ-S curves for the position 37° 05'N, 122° 47'W, 37 km off Point Año Nuevo, California. *Dashed line* is for 16 May 1991; *solid line* is for 13 May 1992.

strong portion of the California Current jet. A strong countercurrent was restored by October 1992.

The anomalous nature of these current patterns is better seen in the differences between the dynamic height and the long-term harmonic mean values for February and July 1992 (figure 10). Except for a small number of stations, these differences are positive, reflecting warmer (less dense) water that occupied the upper 500 m of the water column in 1992. The shading in figure 10 (>6 dynamic cm for February and >10 dynamic cm for July) emphasizes regions of relatively high values and shows that, whereas February had high coastal levels, the relative high in the differences existed as an offshore ridge by July. These differences demonstrate that the coastal countercurrent was stronger than its seasonal mean in February and weaker in July. The inshore poleward countercurrent was again stronger than its seasonal mean in October (not shown). One interpretation is that the anomalous buildup along the coast in February had migrated offshore by July and then been replaced along the coast by a second buildup in fall.

Shore Station Time Series

With a few exceptions, the 1992 anomalies of sea level from the long-term monthly means were positive at San Francisco and San Diego (figure 11). The series confirm the idea that the quarterly CTD surveys sampled an event that cycled roughly over the period between February and October 1992. The largest positive monthly anomaly occurred in March; there was a midyear low and a secondary high in October–November. Coastal sea level has been shown to reflect the geostrophic adjustment of local baroclinic flow (Reid and Mantyla 1976), with high sea level associated with poleward flow. The sequence of monthly sea-level anomalies during 1993 has a more variable pattern, but its largest anomalies still occurred in midwinter (February). In contrast, sea-level anomalies were negative or near zero for much of 1991.

Surface temperatures measured at La Jolla (SIO Pier) and Pacific Grove for 1992 and 1993 were substantially higher than the long-term harmonic mean for much of both years (figure 12). The SST anomalies at La Jolla were near their mean or below it during June–July 1992,

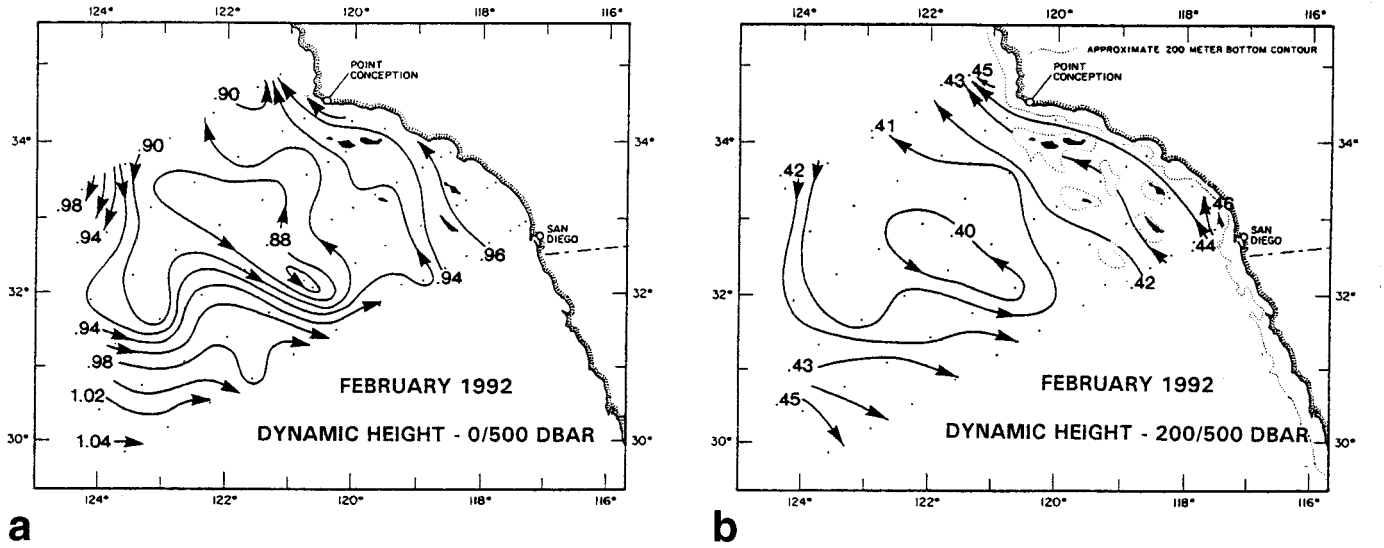

Figure 7. *a*, Dynamic height (dyn. m) of the surface with respect to 500 dbar for CalCOFI survey for 28 January–13 February 1992. Contour interval is .02 dyn. m. *b*, Same as *a*, except showing the 200 m level and with a contour interval of .01 dyn. m.

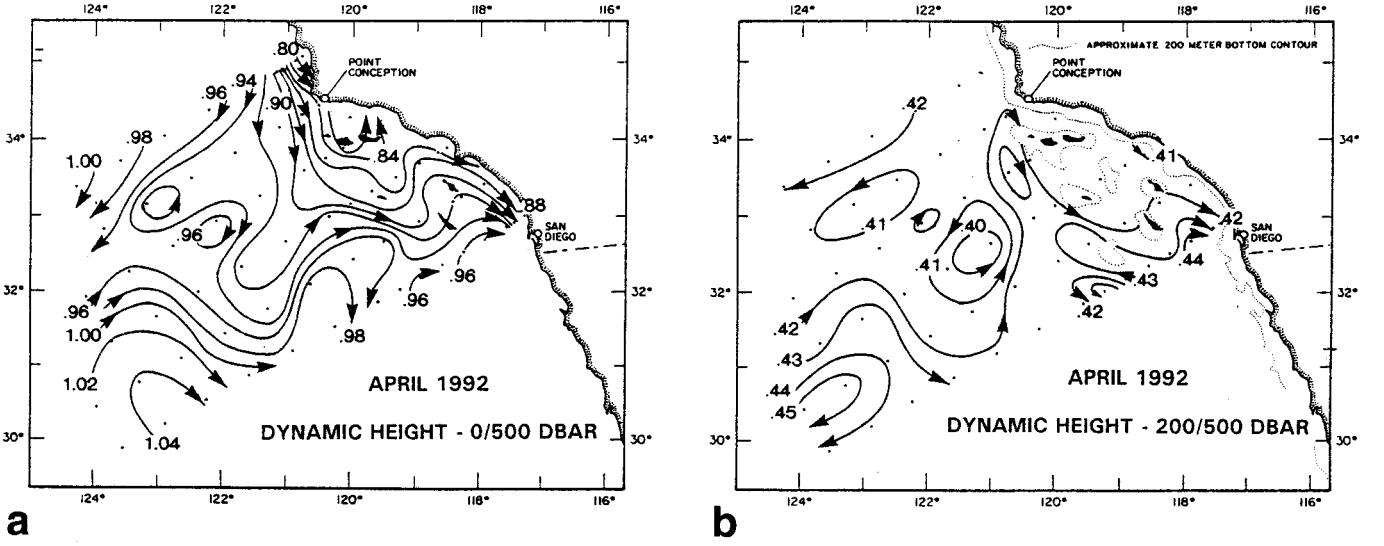

Figure 8. *a*, Dynamic height (dyn. m) of the surface with respect to 500 dbar for CalCOFI survey for 13–30 April 1992. Contour interval is .02 dyn. m. *b*, Same as *a*, except showing the 200 m level and with a contour interval of .01 dyn. m.

a period when San Diego sea-level anomalies were also near their mean. Pacific Grove SST approached near-zero anomalies in August–September 1992, coincident with the smallest San Francisco sea-level anomalies.

Upwelling Index

The time series of standardized anomalies of the Bakun upwelling index (Bakun 1973; Mason and Bakun 1986) between Vancouver Island and Punta Eugenia for 1990–93 (base period 1963–93) is presented in figure 13. Negative upwelling anomalies prevailed without significant interruption during 1992 and 1993 between Point Arena (39°N) and Punta Eugenia (27°N). These anomalies are interpreted as a persistent decrease in coastal upwelling or an increase in downwelling. These anomalies probably led to an increase in sea-surface temperatures above seasonal norms. Persistent alongshore winds that cause coastal upwelling are typical between March and October (figure 14). The anomalously low index values in March 1992 and 1993 indicate a delay in the typical onset of nutrient enrichment of near-surface waters by upwelling, and in the onset of spring plankton blooms. During both years the region between Point Arena and Vancouver Island (51°N) also shows negative upwelling anomalies during late winter and early spring (figure 13).

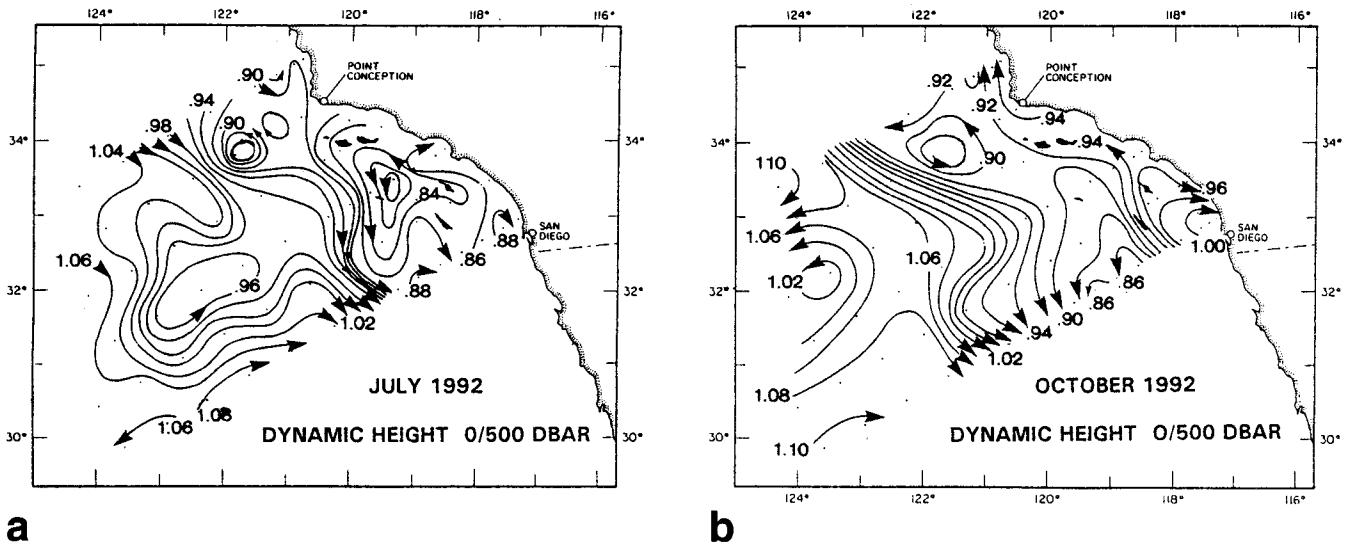

Figure 9. *a*, Dynamic height (dyn. m) of the surface with respect to 500 dbar for CalCOFI survey for 24 July–9 August 1992. Contour interval is .02 dyn. m. *b*, Same as *a*, except showing survey of 28 September–14 October 1992.

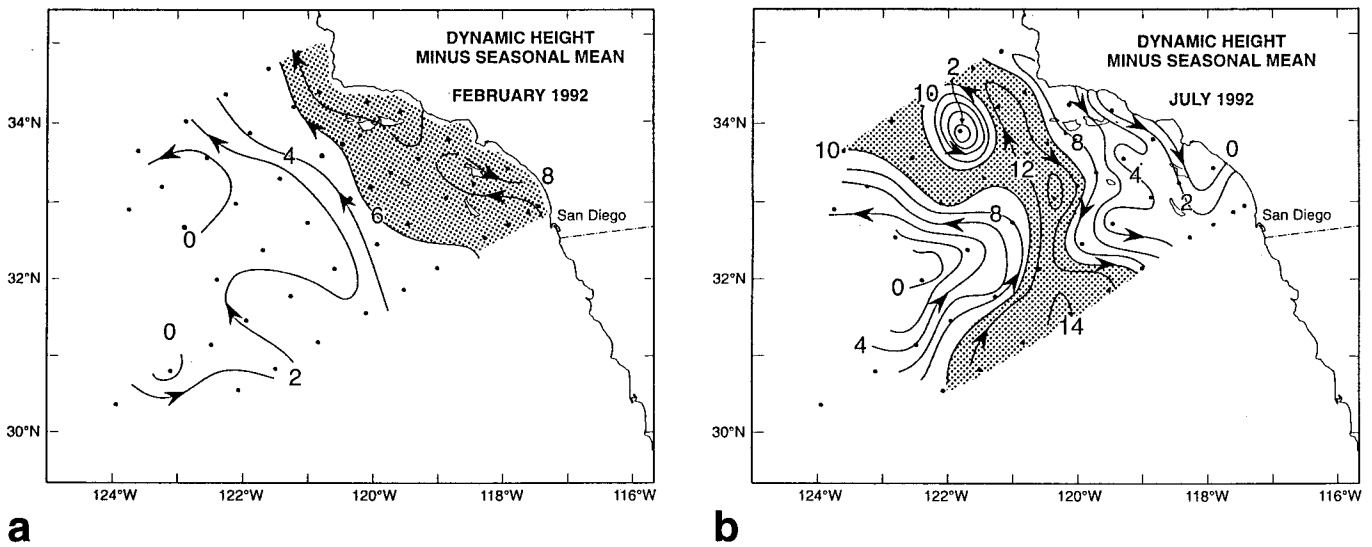

Figure 10. *a*, Dynamic height of figure 7a minus the long-term harmonic mean for February (base period: 1950–92). Contour interval is 2 dyn. cm, and values >6 dyn. cm. are *shaded*. *b*, The dynamic height of figure 9a minus the long-term harmonic mean for July. Values >10 dyn. cm. are *shaded*.

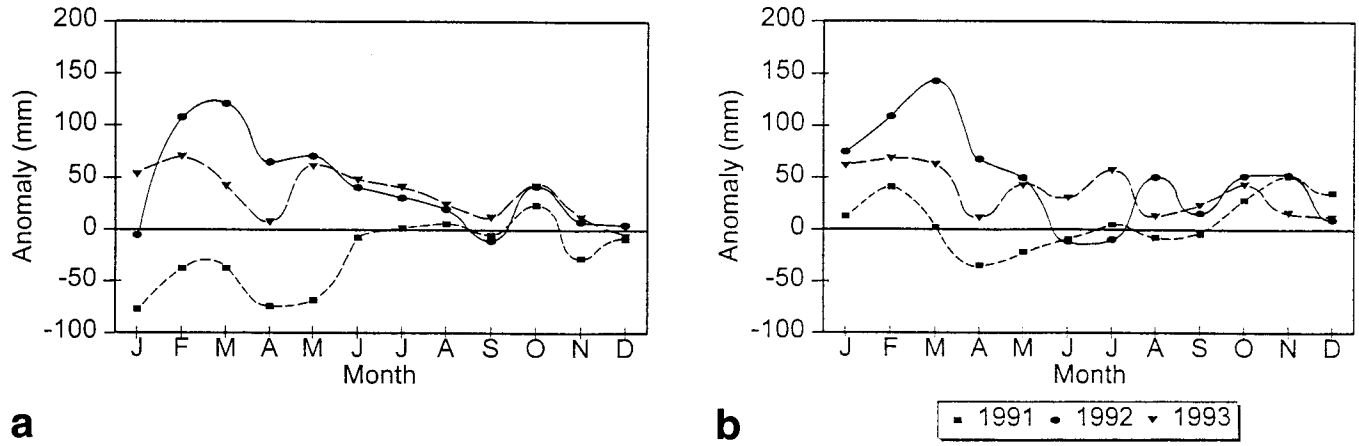

Figure 11. 1991, 1992, and 1993 sea-level anomalies (in mm corrected for atmospheric pressure) from their 1975–86 monthly means for (*a*) San Francisco and (*b*) San Diego. Data provided by the IGOSS program, courtesy of G. Mitchum and K. Wyrtki.

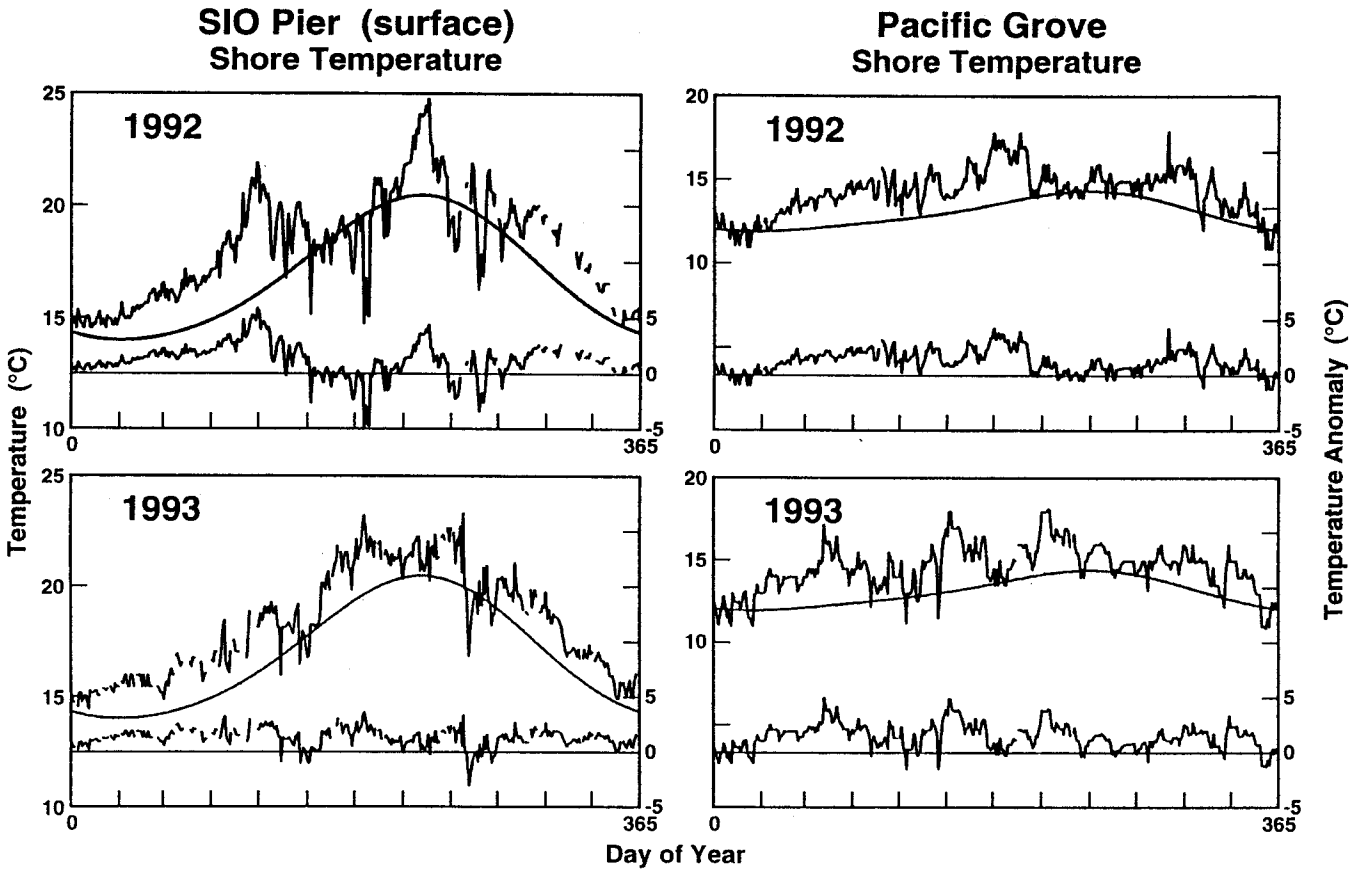

Figure 12. Sea-surface temperature (°C) and its long-term mean annual cycle (*upper curves*) and anomalies (*lower curves*) for the SIO Pier and Pacific Grove for 1992 and 1993 (from Hayward et al. 1994).

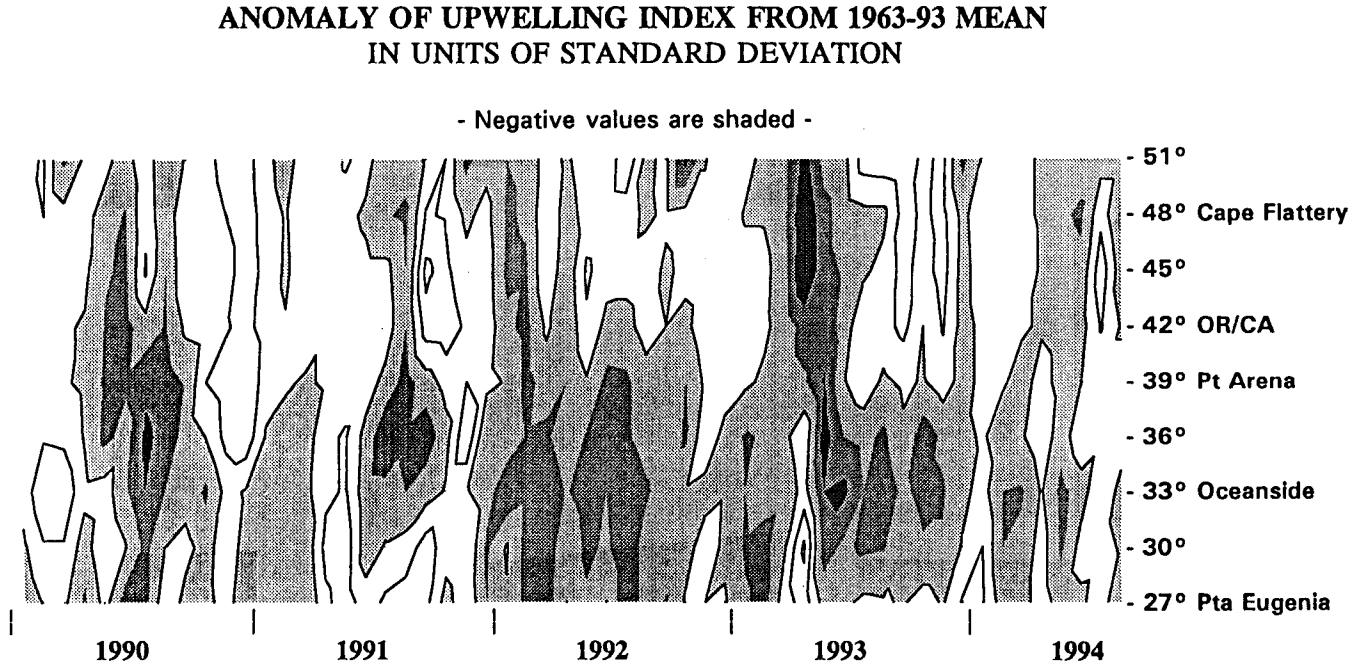

Figure 13. Anomalies of Bakun upwelling index (in standard deviations) from monthly means (base period: 1963–93) for 1990 through July 1994. Negative values (*shaded*) indicate below-normal upwelling or above-normal downwelling. Contour interval is 1 standard deviation.

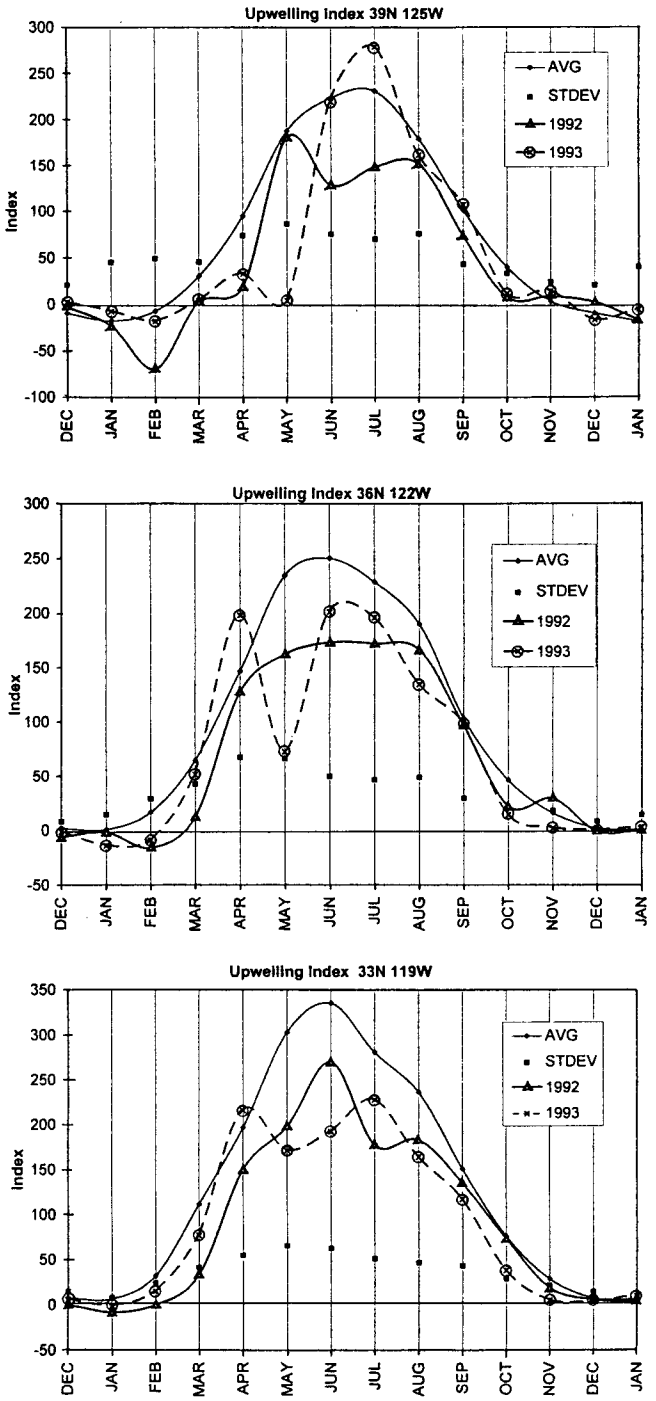

Figure 14. The annual upwelling index for three positions along the California coast as indicated in the key. Units are $m^3/s/100$ m of coastline.

Gradient Winds and Sea-Surface Temperature

This section provides only a cursory treatment of the large-scale meteorological conditions evident during 1991–93 over the North Pacific. A more thorough treatment of this topic is given by Murphree (1995). The March 1992 vector anomalies of 850 mb gradient winds (figure 15) were adapted from the *Climate Diagnostics Bulletin* series, and the SST anomalies from the *Oceanographic Monthly Summary* series. Reference is made to distributions for other months and years given in these publications but not reproduced here.

The seasonality of the winds over the eastern North Pacific is related to the oscillation between the dominance of the Aleutian low-pressure cell (winter) and the Subtropical high-pressure cell (spring and summer). Vector winds were calculated from the pressure distributions. Vector anomalies of 850 mb gradient winds (base period 1979–88) over the North Pacific and including the tropics for March 1992 show two major areas of high values (figure 15a). The eastward-directed vectors between 170°E and 140°W and 10°N and 20°S show that the easterly equatorial trade winds were weakened or reversed, a consequence of anomalous ENSO barometric pressure patterns. This change in the trades generates eastward-propagating equatorial Kelvin waves, decreased equatorial upwelling, and the resulting anomalous equatorial warming.

The other area of highly anomalous wind vectors was found in the eastern North Pacific, where a cusp-shaped contour surrounds anomalous vectors above 5 m/s. Vector anomalies over a large sector of the eastern North Pacific indicate a cyclonic anomaly component in atmospheric circulation. This component was downwelling-favorable along the North American coast. By June 1992, the wind anomalies had decreased, and approached normal seasonal values, but were qualitatively similar to the anomaly patterns in March. The pattern of wind anomalies for March 1993 and 1994 was very similar to March 1992 (although with slightly diminished magnitudes). An enhanced Aleutian low in late winter, followed by an underdeveloped subtropical high, produced similar wind-vector anomalies during winter and spring in 1992, 1993, and 1994.

The SST anomaly distribution for March 1992 (Figure 15b) forms a basinwide pattern. Positive values occurred in a broad sweep across the tropics, along a broad region off the North American continent, and down the Kamchatka Peninsula to Japan; a large body of the central North Pacific is negative. This general pattern of anomalous SST dominated most of 1992 and the first half of 1993. The equatorial SST anomalies returned to near zero and went negative after June 1993, but the large field of positive anomalies returned in the eastern North Pacific and persisted to June 1994.

DISCUSSION

The development of a strong and broad countercurrent/undercurrent during March and April 1992 (figure 1) contrasts sharply with the long-term average baroclinic flow for CalCOFI station line 60 (extending 240°T from Pt. Reyes; Lynn and Simpson 1987). Early spring

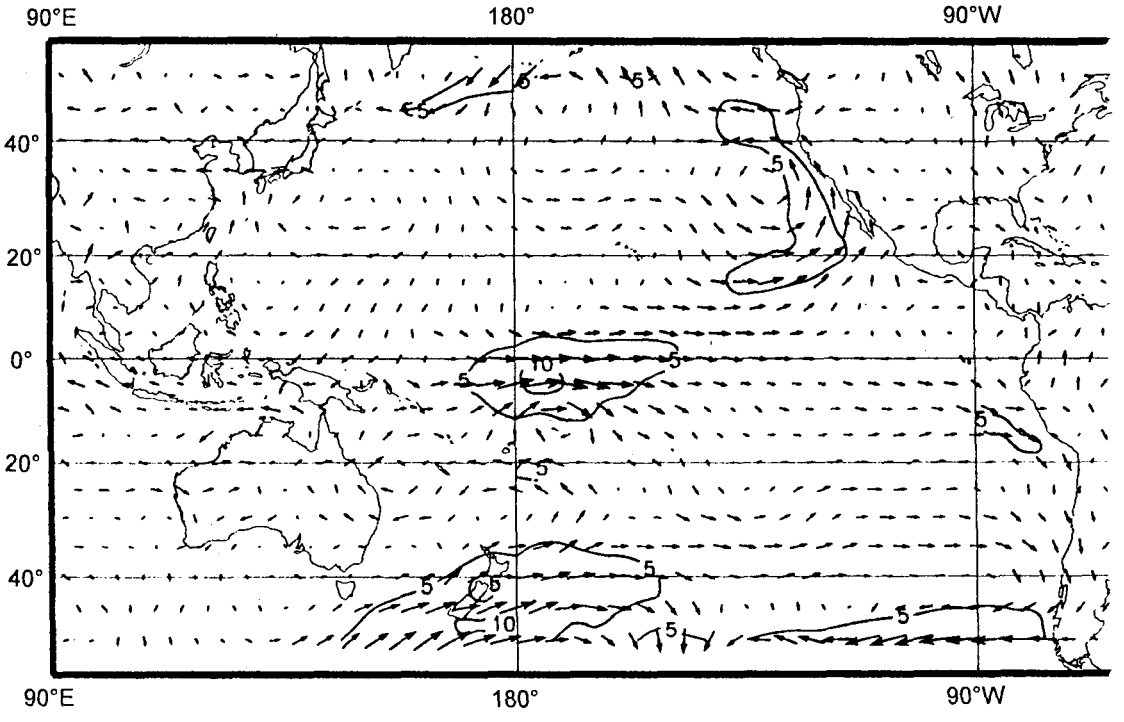

a

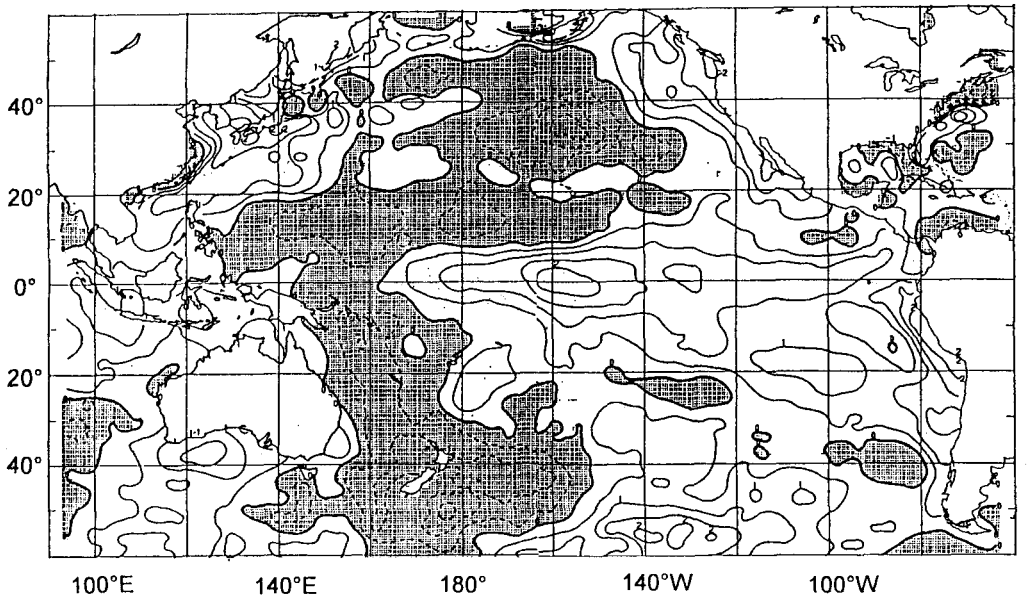

b

Figure 15. *a*, The vector anomalies of 850 mb winds for March 1992 (from *Climate Diagnostics Bulletin*). *b*, the SST anomalies for March 1992 (from *Oceanographic Monthly Summary*). Contour interval is 0.5°C. Negative anomalies are *shaded*.

is typically a period of no poleward flow, when the strongest equatorward flow occurs close to the coast (plate 1 of Lynn and Simpson 1987). As a basis for comparison, this suggests that the 1992 observations depart significantly from the norm. The water-mass distribution (figure 2) supports the findings in current dynamics. It has long been established that the California Undercurrent transports warm, saline, low-oxygen water poleward along the coastal margin (Lynn et al. 1982). The extensive offshore expanse of waters of southerly origin and the development of a strong double gradient in properties on density surfaces are a consequence of the greatly enhanced poleward flow in 1992. The earlier, February surveys show that this strong pattern existed for some

period of time in late winter. The strong poleward flow is equated with high coastal values of dynamic height, matching the anomalously high sea level at San Francisco in that season (figure 11). The disappearance of the Inshore Countercurrent by June (figure 5) matches the decrease in sea-level anomaly.

The sequence of 1992 CalCOFI surveys shows the buildup of an anomalously strong countercurrent/undercurrent off southern California, its collapse, and its return within an eight-month period (figures 7–10). These CalCOFI surveys, like the surveys off central California, are generally descriptive of the major events found in local sea-level measurements. Although the surveys alone are not fully adequate for an unambiguous examination of an intra-annual cycle of events, the agreement between the intermittent measurements of anomalous coastal dynamic height and the continuous measurement of sea level suggests that the surveys are a good representation of the events. The record of sea-level anomaly reflects an exaggerated cycle of anomalous development of the Inshore Countercurrent and California Undercurrent.

The baroclinic adjustment to poleward flow requires a relative downsloping of nearshore density structure. Thus deeper levels generally have higher-than-average temperatures. In terms of the hypothesis of Norton and McLain (1994), an increase in deep (300 m) temperatures correlates with remote forcing, and thus is a consequence of a coastal baroclinic Kelvin wave. The cross-shore length scale of the poleward flow and its anomaly, however, is much broader than internal Kelvin wave theory implies (Mysak 1986). The development of a westward-propagating Rossby wave field (White and Saur 1983) may explain the offshore breadth of the enhanced poleward flow. A Rossby wave moving off the coastal margin would also produce the reversal in the anomalous coastal poleward flow between the February and the July CalCOFI surveys (figure 10). The maximum in dynamic height appears to move offshore over this period.

The large-scale distribution of SST anomalies in March 1992 (Figure 15b) is remarkably similar to that for March 1983 (Oceanographic Monthly Summary; see also Mysak 1986; figure 20); the 1982–83 El Niño was the strongest ever observed. Mysak (1986) and Simpson (1992), among others, conclude that the large-scale SST anomalies characteristic of El Niño and anti–El Niño events are caused by anomalous atmospheric forcing over the North Pacific. Large-scale anomalies in barometric pressure during winter are associated with the subsequent development of SST anomalies. The March 1992 wind-vector anomalies (and the barometric-pressure anomalies from which they were derived) had a length scale proportionate to that of the SST anomalies (figure 15). At their peak, positive SST anomalies extended 1500 km off the California coast.

The anomalous atmospheric circulation alters the wind-driven transport, increasing the poleward flow of the eastern limb of the Alaskan (cyclonic) gyre and decreasing the equatorward flow of the California Current. There is an eastward transport of surface waters toward the California coast (Simpson 1984) and increased vertical mixing in the central North Pacific (Mysak 1986). Anomalous poleward winds along the coast reduce upwelling and increase downwelling. Changes in the wind field could produce changes in Ekman divergence and upwelling over the North Pacific. The altered atmospheric and oceanic circulation and changes in air-sea exchanges result in the large-scale anomalies of SST. The persistence of the anomalous barometric patterns during winter–spring of 1992 and again in winter–spring of 1993 and 1994 provide ample argument that local atmospheric forcing was the dominant factor in the large-scale SST anomalies. But it is not clear that surface-forcing anomalies can account for deep-current and water-mass perturbations.

The cycle of the development of a relative coastal high in dynamic height, its offshore migration, and its reinstatement along the coast described here for 1992 was also observed in 1958 (Lynn and Reid 1975). In January 1958 there was a relative high in the difference of dynamic height from its long-term harmonic mean (figure 16); a trough was found offshore. The April 1958 distribution had a confused pattern, but by July 1958 the relative high appeared as a ridge off the coast. In October 1958 the relative high was again mostly coastal. This sequence of distributions in anomalous dynamic height describes a stronger-than-normal poleward flow in the coastal zone in January and October, and a stronger-than-normal equatorward flow in July. The SST anomalies were mainly positive during this El Niño event (figure 17); the major exception occurred in July, when anomalous equatorward flow predominated along the coast. The intra-annual cycle of coastal dynamic height revealed by this quartet of surveys is supported by the record of sea-level anomaly for 1958 off San Francisco and La Jolla (figure 18). For reference, the 1983 sea-level anomaly record is also given in figure 18.

Jacobs et al. (1994) applied a global ocean-circulation numerical model (GCM; Hurlburt et al. 1992) of sea-surface height (SSH) to the 1982–83 event. Their figure 2 is a sequence of three maps showing the progression of the simulated deviation of SSH from a 12-year mean for this event. Their results show the buildup of positive SSH anomalies at the equator in August 1982 as a result of the eastward-propagating Kelvin wave. In January 1983, the positive anomaly of SSH stretches northward along the coast to Alaska in response to a coastally trapped

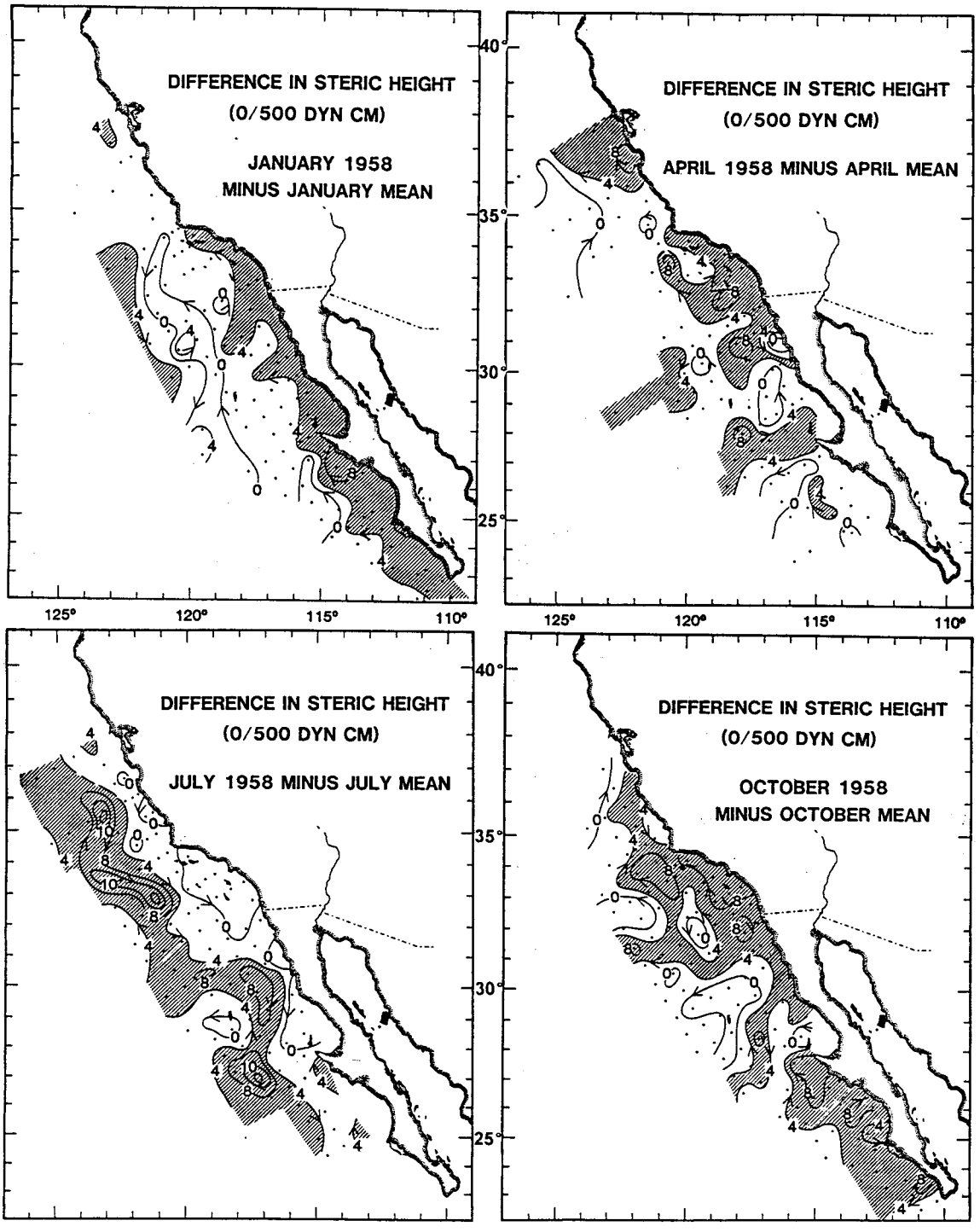

Figure 16. Steric height (same as dynamic height) for four CalCOFI surveys in 1958 minus the monthly harmonic mean steric height (base period: 1950–63). (From Lynn and Reid 1975.) Contour interval is 4 dyn. cm. Values >4 dyn. cm. are *hatched.*

Kelvin wave propagating poleward. Four months later, the signal is carried offshore of the North American continent as a westward-propagating Rossby wave; the positive SSH anomaly appears as an offshore ridge. These simulated distributions of SSH represent changes in circulation like those given by the observed differences of dynamic height from its long-term mean. The coastal high in model SSH anomalies for January would geostrophically balance an anomalous poleward flow. The ridge in SSH found for May 1983 would balance an anomalous equatorward flow on its shoreward side. The numerical model results closely resemble the

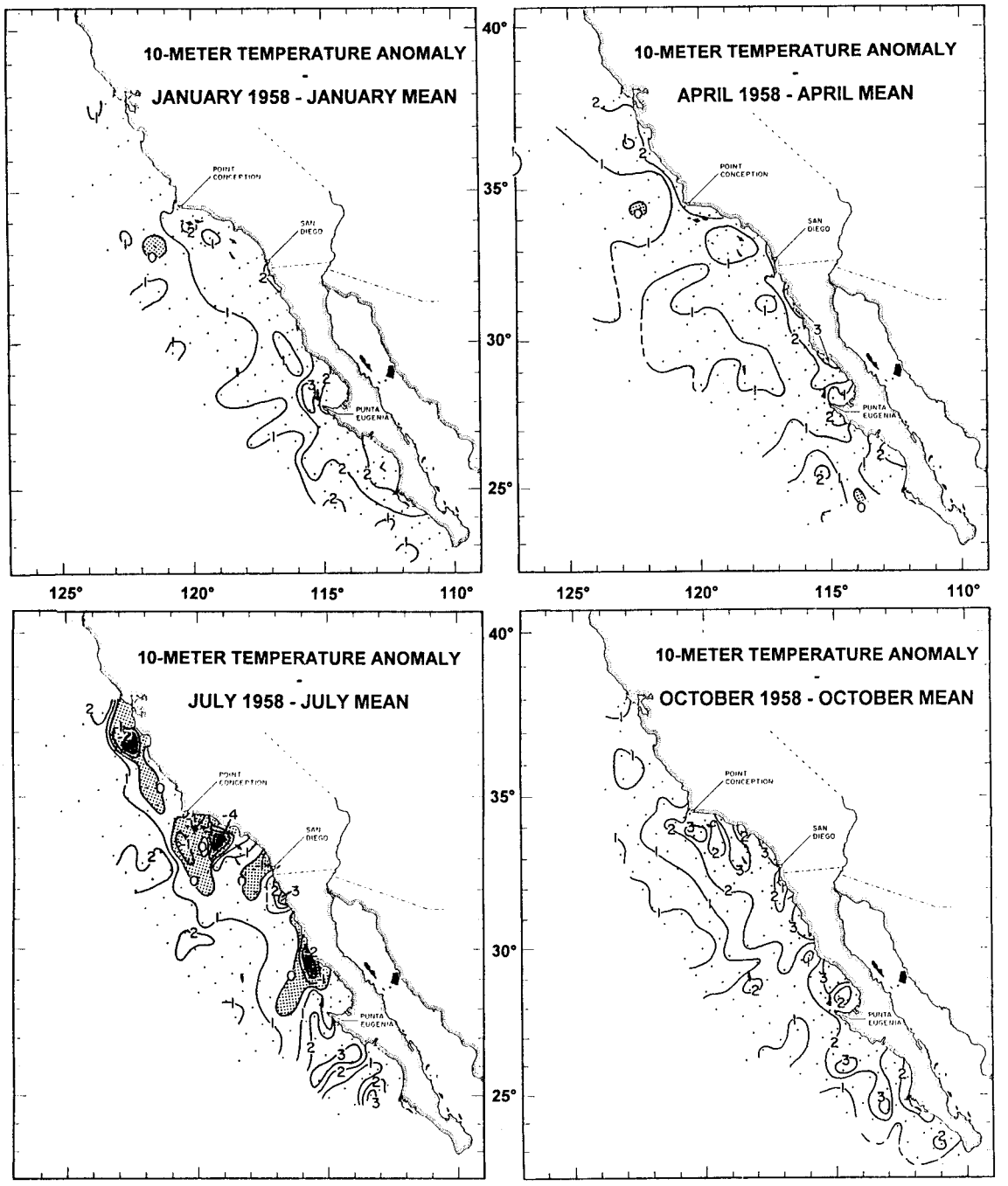

Figure 17. SST anomalies for the four surveys of figure 16 (from Lynn and Reid 1975). Negative values are *shaded*.

anomalous patterns of dynamic height found during 1958 (figure 16) and 1992 (figure 10) and thus provide an argument that some of the dynamical response of eastern North Pacific El Niño events is a consequence of modified Kelvin wave/Rossby wave forcing.

Researchers from the Los Alamos National Laboratory and the Naval Postgraduate School have simulated SSH and barotropic currents from January 1985 through June 1994, using a different GCM (Julie McClean, pers. comm.). Model SSH anomalies of about 20 cm and barotropic transport anomalies of 100 m^2/sec propagated poleward along the coast of North America from January through April 1992. The researchers conclude that the anomalously strong signal in 1992 is the poleward-propagating extension of equatorial Kelvin waves resulting from the 1991 El Niño event. They also note SSH anomalies propagating westward from the coastal region in April 1992, consistent with Rossby wave

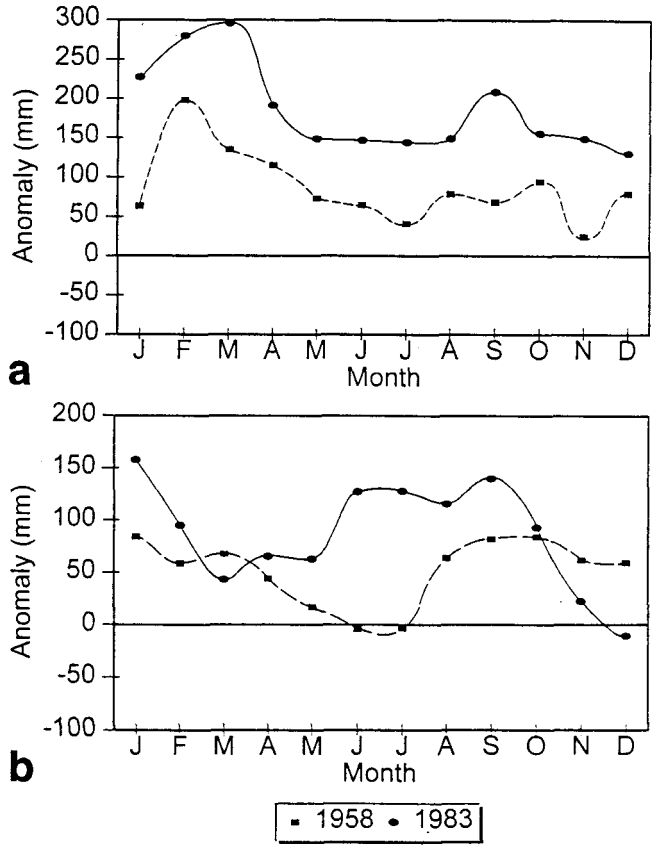

Figure 18. 1958 and 1983 sea-level anomalies (in mm) from the monthly means for (*a*) San Francisco (1900–92) and (*b*) La Jolla (1925–92). The secular trend has been removed from both sets.

development. We hope that the observations described in this report will stimulate further theoretical studies of the mechanism that produces oceanic anomalies off North America during El Niño events.

CONCLUSIONS

We speculate that the observed El Niño signal in the eastern North Pacific is some combination of anomalous local atmospheric forcing (which has its strongest influence in the upper ocean) and remotely generated oceanic perturbations (which likely propagate as coastally trapped waves and apparently are most evident at mid-depths within an internal Rossby radius of the coast). The dominant forcing that produces the enhanced and unseasonal Inshore Countercurrent remains unclear, although its occurrence in late winter during ENSO events is apparent. The suggestion is raised that the delay in spring transition to an upwelling regime, coupled with reduced upwelling (increased downwelling), large-scale onshore transport, and Kelvin wave dynamics may all play a part in the observed anomalous conditions in the California Current system. Comparative evidence with models suggests that the development of a Rossby wave may account for an offshore migration of a high ridge in anomalous sea-surface elevation, relating to a return to equatorward coastal circulation. The large-scale patterns of SST anomalies, however, are of such magnitude, extent, and persistence over this period that they are clearly attributed to anomalous atmospheric forcing.

An ENSO event began developing in the Pacific equatorial zone in mid-1994 and reached maturity by year's end (*Climate Diagnostics Bulletins* 1994). The large-scale SST pattern of the North Pacific for December 1994 is opposite to that often described as the typical El Niño north event (e.g., figure 15b). The central North Pacific has a large region of positive SST anomaly, and the North American coastal region is negative. However, the January 1995 *El Niño Watch Advisory* (issue 95-1, CoastWatch, SWFSC, La Jolla) shows recent coastal warming; the near-coastal waters as of mid-January were close to 1°C above their long-term mean. The ensuing degree of response of local waters will contribute to our understanding of the forcing mechanisms. A continuous monitoring system established at various positions along the coast within the water column would help to provide the unambiguous answer.

ACKNOWLEDGMENTS

We thank the scientific and technical staffs, both past and present, of the CalCOFI program; the personnel of the Southwest Fisheries Science Center involved in the FORAGE program at La Jolla (under the leadership of R. M. Laurs) and the Groundfish Analysis Investigations (under the leadership of W. H. Lenarz and S. Ralston); and other unnamed individuals involved in collecting the many sources of data that we have used. Processing and quality control of 1992–93 CTD data were handled by K. Bliss, A. Mantyla, and K. Sakuma. H. Parker provided the upwelling index data. We also thank Jane Huyer and an anonymous reviewer for very helpful suggestions that improved the manuscript.

LITERATURE CITED

Bakun, A. 1973. Coastal upwelling indices, west coast of North America 1946–71. U. S. Dep. Commer. NOAA Tech. Rep. NMFS SSRF-671, 103 pp.

Chelton, D. B., and R. E. Davis. 1982. Monthly mean sea-level variability along the west coast of North America. J. Phys. Oceanogr. 12:757–784.

Clarke, A. J., and S. Van Gorder. 1994. On ENSO coastal currents and sea level. J. Phys. Oceanogr. 24:661–680.

Climate Diagnostics Bulletin. An ongoing series. U. S. Dep. Commer. NOAA NWS Nat. Meteorol. Center.

Emery, W. J., and K. Hamilton. 1985. Atmospheric forcing of interannual variability in the northeast Pacific Ocean, connections with El Niño. J. Geophys. Res. 90:857–868.

Enfield, D. B., and J. S. Allen. 1980. On the structure and dynamics of monthly mean sea level anomalies along the Pacific coast of North and South America. J. Phys. Oceanogr. 10:557–578.

Hayward, T. L. 1993. Preliminary observations of the 1991–1992 El Niño in the California Current. Calif. Coop. Oceanic Fish. Invest. Rep. 34:21–29.

Hayward, T. L., A. W. Mantyla, R. J. Lynn, P. E. Smith, and T. K. Chereskin. 1994. The state of the California Current in 1993–1994. Calif. Coop. Oceanic Fish. Invest. Rep. 35:19–35.

Hayward, T. L., D. R. Cayan, P. Franks, R. J. Lynn, A. W. Mantyla, J. A. McGowan, P. E. Smith, F. B. Schwing, and E. L. Venrick. 1995. The state of the California Current in 1994–1995: a period of transition. Calif. Coop. Oceanic Fish. Invest. Rep. 36 (this volume).

Horel, J. D., and J. M. Wallace. 1981. Planetary-scale atmospheric phenomena associated with the Southern Oscillation. Monthly Weather Rev. 109:813–829.

Hurlburt, H. E., A. J. Wallcraft, Z. Sikes, and E. J. Metzger. 1992. Modeling of the Global and Pacific Oceans: on the path to eddy-resolving ocean prediction. J. Oceanogr. 5:9–18.

Huyer, A., and CTZ colleagues. 1991. Currents and water masses of the coastal transition zone off northern California, June to August 1988. J. Geophys. Res. 96:14,809–14,832.

Jacobs, G. A., H. E. Hurlburt, J. C. Kindle, E. J. Metzger, J. L. Mitchell, W. J. Teague, and A. J. Wallcraft. 1994. Decade-scale trans-Pacific propagation and warming effects of an El Niño anomaly. Nature 370:360–363.

Jessen, P. F., S. R. Ramp, L. K. Rosenfeld, C. A. Collins, N. Garfield, and F. B. Schwing. 1992. Hydrographic and acoustic Doppler current profiler (ADCP) data from the Farallones shelf and slope study, 7–17 February 1992, Naval Postgrad. Sch. Tech. Rep. NPS-OC-92-005. 139 pp.

Latif, M., and T. P. Barnett. 1994. Causes of decadal climate variability over the North Pacific and North America. Science 266:634–637.

Lynn, R. J., and J. L. Reid. 1975. On the year to year differences in the characteristics of the California Current. Abstracts of papers, Thirteenth Pac. Sci. Congr. Pac. Sci. Assoc. (abstract only), p. 261.

Lynn, R. J., and J. J. Simpson. 1987. The California Current system: the seasonal variability of its physical characteristics. J. Geophys. Res. 92:12,947–12,966.

Lynn, R. J., K. A. Bliss, and L. E. Eber. 1982. Vertical and horizontal distributions of seasonal mean temperature, salinity, sigma-t, stability, dynamic height, oxygen, and oxygen saturation in the California Current, 1950–1978, Calif. Coop. Oceanic Fish. Invest. Atlas 30, Univ. Calif. San Diego, 513 pp.

Mason, J. E., and A. Bakun. 1986. Upwelling index update, U. S. west coast, 33N–48N latitude. U. S. Dep. Commer. NOAA Tech. Memo. NOAA-TM-NMFS-SWFSC-67, 81 pp.

Mysak, L. A. 1986. El Niño, interannual variability and fisheries in the northeast Pacific Ocean. Can. J. Fish. Aquat. Sci. 43:464–497.

Murphree, T., and C. Reynolds. 1995. El Niño and La Niña effects on the northeast Pacific: the 1991–1993 and 1988–1989 events. Calif. Coop. Oceanic Fish. Invest. Rep. 36 (this volume).

Norton, J. G., and D. R. McLain. 1994. Diagnostic patterns of seasonal and interannual temperature variation off the west coast of the United States: local and remote large-scale atmospheric forcing. J. Geophys. Res. 99:16,019–16,030.

Oceanographic Monthly Summary. An ongoing series. U. S. Dep. Comm. NOAA/NOS/NWS and /NESDIS.

Ramp, S. R., N. Garfield, C. A. Collins, L. K. Rosenfeld, and F. B. Schwing. 1992. Circulation studies over the continental shelf and slope near the Farallon Islands, CA. Executive Summary. U.S. Environmental Protection Agency and the Western Division, Naval Facilities Engineering Command, 22 pp. + figs.

Reid, J. R., and A. W. Mantyla. 1976. The effect of the geostrophic flow upon coastal sea level variations in the northern Pacific Ocean. J. Geophys. Res. 81:3100–3110.

Sakuma, K. M., H. A. Parker, S. Ralston, F. B. Schwing, D. M. Husby, and E. M. Armstrong. 1994a. The physical oceanography off the central California coast during February–March and May–June, 1992: a summary of CTD data from pelagic young-of-the-year rockfish surveys. U.S. Dep. of Comm., NOAA Tech. Mem. NOAA-TM-NMFS-SWFSC-208, La Jolla, Calif. 169 pp.

———. 1994b. The physical oceanography off the central California coast during February–March and May–June, 1993: a summary of CTD data from pelagic young-of-the-year rockfish surveys. U.S. Dep. of Comm., NOAA Tech. Mem. NOAA-TM-NMFS-SWFSC-209, La Jolla, Calif. 174 pp.

Simpson, J. J. 1983. Large-scale thermal anomalies in the California Current during the 1982–1983 El Niño. Geophys. Res. Lett. 10:937–940.

———. 1984. A simple model of the 1982–83 Californian "El Niño." Geophys. Res. Lett. 11:237–240.

———. 1992. Response of the southern California current system to the mid-latitude North Pacific coastal warming events of 1982–1983 and 1940–1941. Fish. Oceanogr. 1:57–79.

SIO. Scripps Institution of Oceanography. 1992a. Physical, chemical, and biological data report. CalCOFI cruises 9108, 9110. SIO Ref. 92-16.

———. 1992b. Physical, chemical, and biological data report. CalCOFI cruises 9202, 9204. SIO Ref. 92-20.

———. 1993. Physical, chemical, and biological data report. CalCOFI cruises 9301, 9304. SIO Ref. 93-26.

———. 1994. Physical, chemical, and biological data report. CalCOFI cruises 9308, 9310. SIO Ref. 94-14.

Strub, P. T., P. M. Kosro, and A. Huyer. 1991. The nature of the cold filaments in the California Current system. J. Geophys. Res. 96:14,743–14,768.

White, W. B., and J. F. T. Saur. 1983. Sources of interannual baroclinic waves in the eastern subtropical North Pacific. J. Phys. Oceanogr. 13:531–544.

Wooster, W. S., and D. L. Fluharty, eds. 1985. El Niño north. Seattle: Univ. Wash. 312 pp.